Title

Discovery of davemaoite, CaSiO3-perovskite, as a mineral from the lower mantle

Journal

Science, 374(6569)

ISSN

0036-8075

Authors

Tschauner, Oliver
Huang, Shichun
Yang, Shuying
et al.

Publication Date

2021-11-12

DOI

10.1126/science.abl8568

Peer reviewed

Title: Discovery of davemaoite, $CaSiO_3$-perovskite as a mineral from the lower mantle

One sentence summary: Davemaoite, natural $CaSiO_3$-perovskite provides evidence for thermo-chemical segregation in the lower mantle.

Authors: Oliver Tschauner[1*], Shichun Huang[1], Shuying Yang[2], Munir Humayun[2], Wenjun Liu[3], Stephanie N. Gilbert Corder[4], Hans A. Bechtel[4], Jon Tischler[3], George R. Rossman[5]

Affiliations:

1. Department of Geoscience, University of Nevada Las Vegas.
2. National High Magnetic Field Laboratory and Department of Earth, Ocean & Atmospheric Science, Florida State University, Tallahassee, FL 32310, USA.
3. Advanced Photon Source, Argonne National Laboratory, Lemont, IL 60439, USA.
4. Advanced Light Source, Lawrence Berkeley National Laboratory, Berkeley, CA 94720, USA.
5. Division of Geological and Planetary Sciences, California Institute of Technology, Pasadena, CA 91105, USA.

*Correspondence to: oliver.tschauner@ unlv.edu

Abstract:

Calcium silicate perovskite, $CaSiO_3$, is arguably the geochemically most important phase in the lower mantle, because it concentrates elements that are incompatible in the upper mantle, including the heat generating elements Th, and U, which have half-lives longer than the geologic history of the Earth. We report $CaSiO_3$-perovskite as an approved mineral (IMA2020-12a) with the name davemaoite. The natural specimen of davemaoite proves the existence of compositional heterogeneity within the lower mantle. Our observations indicate that davemaoite also hosts K in addition to U and Th in its structure. Hence, the regional and global abundances of davemaoite influence the heat budget of the deep mantle, where the mineral is thermodynamically stable.

Main text:

Calcium silicate, $CaSiO_3$, occurs in a variety of natural and synthetic polymorphs. The low-pressure polymorph wollastonite is a common metamorphic mineral. Breyite *(1)*, an intermediate-pressure polymorph *(2)*, has been found as inclusions in diamond. At the pressures and depth range of the Earth's transition zone (TZ, 420-660 km) and lower mantle (LM, 660 to about 2700 km) $CaSiO_3$ assumes a perovskite-structure. Perovskite-type $CaSiO_3$ was first synthesized by Liu and Ringwood (*3*) and is a liquidus phase for basaltic and peridotic bulk rock compositions at LM pressures and temperatures, and has been experimentally shown to host many elements that are incompatible in upper mantle minerals (*4-7*). These include rare earth

elements (REEs), large ion lithophile elements (K,Sr, Ba) (LILEs), Ti, U, and Th. In other words, these elements are compatible rather than incompatible in a LM mineral assemblage that contains a few vol-% of $CaSiO_3$-perovskite. The composition and abundance of this phase in the LM are, therefore, key in constraining the budget and distribution of REEs and LILEs and the elements with abundant radioactive isotopes (K, U, Th) that make an important contribution to the heat of the Earth's mantle (*8*). Through these parameters $CaSiO_3$-perovskite provides essential constraints on the fate of recycled crust in the deep Earth, thermo-chemical anomalies, and the existence of a magma ocean at the base of the Earth's mantle. The synthetic perovskite phase of pure $CaSiO_3$ has been found to assume either cubic or tetragonal symmetry (*9*) and belongs to the tausonite ($SrTiO_3$)-type of perovskites that adhere to fundamentally different structural distortion mechanisms (*10*) and crystal-chemical constraints than the $GdFeO_3$-type perovskites like bridgmanite ($MgSiO_3$-perovskite, ref. *11*) and the $CaTiO_3$ mineral, actually named perovskite.

The difficulty in finding $CaSiO_3$-perovskite in nature is due to its stability at pressures only above 20 GPa (*3,4*) along with a low kinetic barrier for back-conversion into low pressure polymorphs (*2*). This barrier is lower than for bridgmanite, which has been found as a rare occurrence in highly shocked meteorites despite its stability only above 23 GPa (*11,12*). Nestola et al. (*13*) reported the presence of $CaSiO_3$-perovskite as an inclusion in a diamond from the Cullinan mine, South Africa. The reported phase deviates from synthetic $CaSiO_3$-perovskite in several ways, (i) its volume at ambient conditions is > 20% larger (*9*), (ii) it sustains the beam of an electron microscope whereas any synthetic $CaSiO_3$-perovskite vitrifies rapidly at ambient conditions, (iii) its cell axis ratios and Raman-spectrum are nearly equal to those of $CaTiO_3$, and (iv) its space

group indicates a structural distortion mechanism different from those of synthetic $CaSiO_3$-perovskite but much closer to $CaTiO_3$ (*7,8*). Nestola et al. (*13*) proposed that this unique phase of $CaSiO_3$ is the result of partial decomposition of a Ti-bearing $CaSiO_3$-perovskite. The coexistence of $CaTiO_3$ + $CaSiO_3$ polymorphs in diamond inclusions may also point to retrograde transformation of stoichiometric Ca-Si-Ti-perovskites (*1*) that form in the deep upper mantle (5-10 GPa).

The findings by Nestola et al. (*13*) are interesting by themselves but different from the expected high pressure $CaSiO_3$-perovskite and have not resulted in the approval of $CaSiO_3$-perovskite as a mineral. We report the discovery of $CaSiO_3$-perovskite as a mineral approved by the Commission of New Minerals, Nomenclature, and Classification (CNMNC) of the International Mineralogical Association (IMA). The new mineral (IMA2020-012a, ref. *14*) is named davemaoite in honour of Dave (Ho-kwang) Mao for his eminent contributions in the field of deep mantle geophysics and petrology. The type material, inclusions in a diamond from Orapa, Botswana, is deposited in the Natural History Museum Los Angeles (catalogue number NHMLA 74541, formerly GRR1507 of the Caltech mineral collection, *15*). Davemaoite coexists with orthorhombic carbonaceous α-iron, and wüstite $(Fe_{0.8}Mg_{0.2})O$ at 8-9 GPa remnant pressure (Fig. 1). Separate inclusions of ilmenite, iron, and ice-VII in the same diamond (*16*) have remnant pressures of 7 GPa and 8-9 GPa, respectively. The X-ray diffraction (XRD) pattern of davemaoite is that of a cubic perovskite (Fig. 1, *15*), at most with contributions of <5 vol% of material with ±2.5% smaller or larger volume, whereas an overall distortion of the lattice can be excluded based on the reflection intensities (Fig 1). Cubic ABO_3 perovskites have no internal structural degrees of freedom and comprise only one chemical formula unit. Thus, the

identification of this phase is unambiguous even in diffraction patterns with contributions from more than one phase (Fig. 1).

Davemaoite was identified through the XRD pattern of cubic perovskite at a location in the hosting diamond with a Ca-kα X-ray fluorescence (XRF) signal far above background. Both, XRF and XRD data were obtained at beamline 34-IDE at the Advanced Photon Source (*15*). We superimposed the Ca-kα XRF map (Fig. 2) on a visible light image of the holotype material at the beamline where we subsequently collected the XRF and XRD data. We also made corresponding maps of Fe and Ti (Fig. S1). Areas with XRF signal at noise level in Fig. 2 show no X-ray diffraction besides that of diamond. Right after acquisition of the XRF map we examined by XRD the inclusions that were found by XRF. XRD and XRF were collected on the inclusions when they were fully entrapped in the doubly polished platelet of the hosting diamond. We focused the X-ray beam to 0.5×0.5 μm^2 in order to identify inclusions with high spatial resolution. The inclusions of 4×6 and 4×16 μm^2 area within the red circle of the Ca XRF map corresponded to the XRD patterns of the cubic perovskite (Fig 1). We added frames with perovskite-patterns in order to obtain better signal and powder statistics.

We confirmed the identification of davemaoite by infrared spectroscopy. Cubic ABO_3 perovskites have no Raman-active and three infrared (IR)-active modes (*15*). We observe two of the three IR-active modes (Fig 1, insert), while the third one is below the diffraction limit for objects as small as these inclusions. As expected, we observed no Raman-peaks (Fig. S2). We calculated mode energies by fitting force constants to match ab initio calculated zone-center phonon energies of the tetragonal structure (*18*) and mapped onto the cubic structure. Intensities are based on the calculated phonon density of state.

Subsequently, we used laser-ablation inductively coupled mass spectrometry (LA-ICP-MS) to excavate and analyze the chemical compositions of two of the inclusions with a 100 μm diameter laser beam. We indicate the ablation area with a red circle (Fig. 2). We monitored all mass peaks under medium mass resolution ($m/\Delta m = 4{,}000$), which allowed us to resolve numerous carbon-related molecular interferences on low-mass isotopes. We hit two inclusions of davemaoite at 5-8 μm and 80-100 μm depth below the polished surface (Fig. 2, insert). The time-resolved ^{44}Ca signal of the LA-ICP-MS measurement (Fig 2 insert) shows signal clearly above background level. We also collected equivalent profiles for ^{56}Fe, ^{39}K, and ^{52}Cr (Fig. S1). In all cases the signals rose above background at the same depth consistent with their origin in the same two inclusions. We obtained an average davemaoite composition of $(Ca_{0.43(1)}K_{0.20(1)}Na_{0.06}Fe_{0.11(1)}Al_{0.08}Mg_{0.06}Cr_{0.04(2)})(Si_{1.0(2)}Al_{0.00(1)})O_3$ (*15*). We performed aRietveld refinement (Fig. 1) and provide a crystallographic information file (*15*).

We describe the hosting diamond, and then discuss the pressure-temperature conditions of formation of the type davemaoite and its composition. The hosting diamond is different from diamonds that contain potential retrograde products of high-pressure minerals at zero to 1 GPa remnant pressures (*13,19*). The diamond is of type IaAB with frosted octahedral faces and trigon-features (*15*). We found davemaoite, iron, wüstite, ilmenite, and ice-VII in the center of the diamond. Our analysis of the N-defect IR bands (Fig. S3, ref. *12*) indicates a low average residence temperature (~1500 K) or a short residence time in the mantle, similar to the holo- and cotype diamonds of ice-VII (*19*). Short residence time and low average residence temperature are common features of lithospheric diamonds, but in sublithospheric diamonds both parameters act in favor of conserving high remnant pressures and high-pressure minerals by reducing

viscoelastic relaxation of the hosting diamond and by preventing retrograde transformations. The bulk modulus of davemaoite depends on its composition (*7,8*), which we don't know because of the lack of compression data for the given composition. However, coexisting wüstite is at a remnant pressure of 8-9 GPa (*16*). For a single inclusion of wüstite this remnant pressure would correspond to an entrapment pressure of ~ 40 GPa if pressure would evolve along a purely elastic path (*15*). However, diamond becomes viscoelastic between 1100 and1200 K even at laboratory time-scales (*20*). In order to account for this non-elastic behavior of the hosting diamond we use the method of Wang et al. (*21*) that does not rely on initial assumptions about the entrapment temperature and uses the P-T paths of separate inclusions in the same diamond: wüstite, iron, ice-VII, and ilmenite. Based on this approach we assessed entrapment conditions of 29 ± 5 GPa at 1400-1600 K (*15*). Because viscoelastic processes are path- and time-dependent of we cannot exclude a higher entrapment-pressure or -temperature.

We cannot entirely exclude that our chemical analysis is affected by minor contaminants, although we did not observe either XRD signal or marked XRF signal of any phase other than davemaoite, wüstite, and iron in the excavated region. However, (i) the low Ti is a result unaffected by potential contamination, and (ii) the ^{39}K signal occurs at the same depth as the ^{44}Ca signal of davemaoite. We did not observe by XRD alternative hosts of K and Ca such as liebermannite and hatrumite-type $(Ca,K,Na)(Al,Si)_2O_4$ anywhere in this diamond. Both of these phases, and any phase dominated by K and Ca, give diffraction patterns that are very different from the perovskite-type pattern we observed. Hence, we believe the presence of K and Al in davemaoite is not likely the result of a contaminated analysis but indicates coupled substitution of a large and a small cation K, Na + Al,Fe for Ca. We note that the partial substitution of K for

Ca and Al for Si shifts the material into the stability field of ABO_3-perovskites with a trend towards high crystal symmetry (*22*).

Our result indicates that the post-spinel phase $(Ca,Na,K)(Al,Si)_2O_4$ is not required as a host of Ca, alkalis, and Al in at least the upper region of the lower mantle. It is possible that type-davemaoite formed retrograde out of post-spinel through a reaction $(Ca,Na,K)(Al,Fe^{3+}, Si)_2O_4 + Fe^0 \rightarrow (Ca,Na,K)(Al,Si)O_3 + FeO$ but for this process one expects the presence of remnant postspinel in the paragenesis and this is not observed. In the deep mantle, davemaoite takes a role similar to that of garnet in the upper mantle. Both minerals have a 'garbage can' crystal chemistry that allows them to host many elements that are incompatible in upper mantle minerals (*6,7*). Our observations are fully consistent with the experimental results that this mineral dissolves LILEs, in particular K (*6,7*). Experimental studies that were based on peridotite and MORB(mid-ocean ridge-basalt)-like bulk compositions formed davemaoite with lower K- and a higher Ti- contents than the type material, which is expected for these starting compositions. We argue that the low Ti- and high K content of type davemaoite reflect a different, K-rich source composition, possibly as result of deep mantle metasomatism that is also indicated by the presence of ice-VII and by the hosting diamond itself (*16*). This point emphasizes the importance of studying natural specimens of high-pressure minerals, because they record a petrologic complexity of the deep Earth that may not be assessed in experiments. Depletion of Ti in type davemaoite is a possible result of the presence of phases that strongly partition Ti, such as liuite, $FeTiO_3$-perovskite. Ilmenite has been observed in the same diamond at similar remnant pressure as the davemaoite-wüstite-iron inclusion and its P-T path intersects the phase boundary of liuite (*15*). Hence, our findings indicate that the source rock composition of type davemaoite deviated from peridotite and, hence, that chemical segregation occurs in the lower mantle possibly down

to 900 km according to our estimate (Fig. S4). This variation in rock composition affects heat generation through radioactive decay in the lower mantle where davemaoite scavenges K as shown here and U +Th as experimentally shown (*7*).

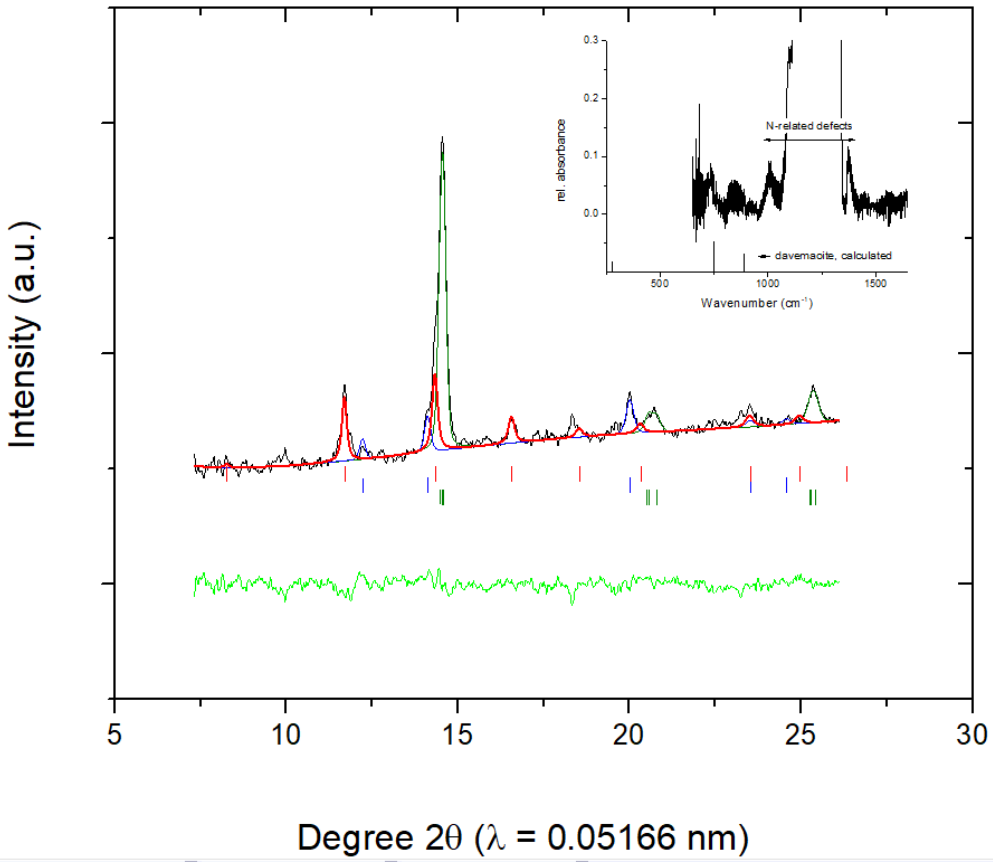

Fig. 1. X-ray diffraction pattern and Rietveld refinement of davemaoite. Red: davemaoite (dvm) olive: (Fe,C), blue: wüstite (wüs), green: residual of fit. Tick marks indicate allowed reflections (same colour-coding). R_{wp} was 0.046 and R_F for dvm was 0.10. Phase proportions were 35(5), 45(5), and 15(5)% for dvm, (FeC), and wüs, respectively. In dvm the intensity of reflections 100 and 201 indicates sublattice disorder of with A-cations shifted from site 1b to the 1/8-occupied site 8g. This is consistent with accommodation of K and Na along with Al and Fe. The paragenesis was found in two inclusions. Volumes of analyzed davemaoite inclusions ranged from 45.1 to 46.3 $Å^3$ (equal to 0 – 6 GPa (*7*) in pure $CaSiO_3$), but the actual composition of davemaoite changes markedly the pressure inferred from the volume (*9*). Coexisting wüstite $Fe_{0.8(1)}Mg_{0.2(1)}O$ has a volume of 74.34(1) $Å^3$, corresponding to 8-9 GPa (*17*). Indications of weak diffraction around dvm peaks near noise level are assigned to minor contributions of material of slightly larger and smaller volume (probably reflecting chemical variation, fit not shown here) but are inconsistent with a tetragonal distortion. Insert: IR spectrum of davemaoite after subtraction of a diamond spectrum collected close to the inclusion. The unprocessed IR spectrum is shown in Fig. S3. Bars indicate all calculated IR-bands.

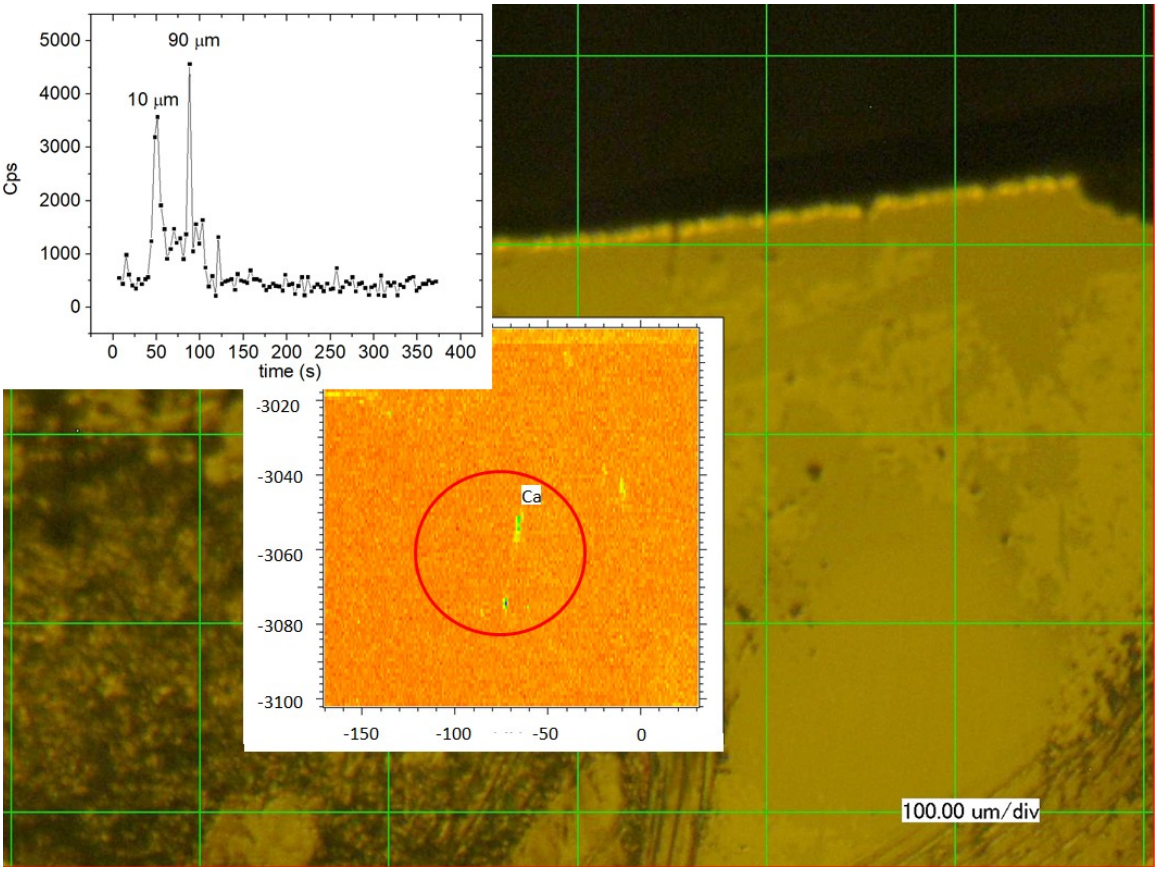

Figure 2: Reflected light image of the diamond at the beamline. The XRF map of CaKα is superimposed. x- and y-axes give the sample coordinates in µm. The red circle indicates the area ablated during LA-ICP-MS analysis. The two Ca-rich areas in the circle correspond to diffraction patterns of davemaoite. The more intense signal around x,y = 72,-3074 corresponds to the shallow inclusion at 8-10 mm depth. Depth was assessed from the attenuation of the XRF signal of Ca and Fe and from the depth of the pit after ablation. Insert: Time-resolved ^{44}Ca signal of LA-ICP-MS measurement. Ablation started at t = 48 s and finished at 108 s.

References and Notes:

1. Brenker, F.E., Nestola. F., Brenker, L., Peruzzo, L., Harris, J.W. Origin, properties and structure of breyite: the second most abundant mineral inclusion in super-deep diamonds. *Am. Min.* **106**, 38-43 (2020).

2. Tschauner, O. High-pressure minerals, *Am. Min.* **104**, 1701-1731 (2019).

3. Liu, L.-g., Ringwood, A.E. Synthesis of a perovskite polymorph of $CaSiO_3$. *Earth Planet. Sci. Lett.* **28**, 209-211(1975).

4. Hirose, K., Sinmyo, R., Hernlund, J. Perovskite in Earth's deep interior. *Science* **358**, 734-738 (2017).

5. Greaux, S., Irifune, T., Higo, Y., Tange, Y., Arimoto, T., Liu, Z.D. , Yamada, A. Sound velocity of $CaSiO_3$ perovskite suggests the presence of basaltic crust in the Earth's lower mantle. *Nature* **565**, 218-220 (2019).

6. Hirose, K., Shimizu, N., van Westrenen, W., Fei, Y.W. Trace element partitioning in Earth's lower mantle and implications for geochemical consequences of partial melting at the core-mantle boundary. *Phys. Earth Planet. Inter.* **146**, 249-260 (2004).

7. Greaux, S., Gautron, L., Andrault, D., Bolfan-Casanova, N., Guignot, N. , Bouhifd, M.A. Experimental high pressure and high temperature study of the incorporation of uranium in Al-rich $CaSiO_3$ perovskite. *Phys. Earth Planet. Inter.* **174**(SI), 254-263 (2009).

8. Korenaga, J. Urey ratio and the structure and evolution of Earth's mantle. *Rev. Geophys.* **46**, RG2007(2008).

9. Chen, H.W., Shim, S.H., Leinenweber, K., Prakapenka, V.B., Meng, Y., Prescher, C. Crystal structure of $CaSiO_3$ perovskite at 28–62 GPa and 300 K under quasi-hydrostatic stress conditions. *Am. Min.* **103**, 462–468 (2018).

10. Glazer, A.M. Simple ways of determining perovskite structures. *Acta Cryst.A* **31**, 756–762 (1975).

11. Tschauner, O., Ma, C., Beckett, J., Prescher, C., Prakapenka, V.B. , Rossman, G.R. Discovery of Bridgmanite – the most abundant mineral in Earth, in a shocked meteorite. *Science* **346**, 1100 – 1102 (2014).

12. Tomioka, N., Fujino, K. Natural $(Mg,Fe)SiO_3$-ilmenite and -perovskite in the Tenham meteorite. *Science* **277**, 1084-1086 (1997).

13. Nestola, F., Korolev, N., Kopylova, M., Rotiroti, N., Pearson, D.G., Pamato, M.G., Alvaro, M., Peruzzo, L., Gurney, J.J., Moore, A.E. , Davidson, J. $CaSiO_3$ perovskite in diamond indicates the recycling of oceanic crust into the lower mantle. *Nature* **555,** 237-241 (2018).

14. Tschauner, O., Huang, S., Yang, S., Humayun, M. Davemaoite, IMA 2020-012a, in: *CNMNC Newsletter* **58**, *Eur. J. Mineral.* **32**, 645 (2020).

15: Materials and methods are available as Supplementary Materials on Science Online

16. Tschauner, O., Huang, S., Greenberg, E., Prakapenka, V. B., Ma, C., Rossman, G. R., Shen, A.H., Zhang, D., Newville, M.G., Lanzirotti, A., Tait, K. Ice-VII inclusions in diamonds – evidence for aqueous fluid in the Earth's deep mantle. *Science* **359**, 1136-1139 (2018).

17. Jacobsen, S. D., Lin, J.F., Angel., R.J., Shen, G.Y., Prakapenka, V.B., Drea, P., Mao, H.K., Hemley, R.J. Single-crystal synchrotron X-ray diffraction study of wustite and magnesiowustite at lower-mantle pressures. *J. Synch. Rad.* **12**, 577-583 (2005).

18. Caracas, R., Wentzcovitch, R., Price, G.D., Brodholt, J. $CaSiO_3$ perovskite at lower mantle pressures. *Geophys Res. Lett.* **32**, L06306 (2005).

19. Stachel, T., Brey, G.P., Harris, J.W. Inclusions in sublithospheric diamonds: Glimpses of deep Earth. *Elements* **1**, 73-78 (2005).

20. Weidner D.J., Vaughan, M.T. Strength of diamond. *Science* **266**, 419-422 (1994).

21. Wang. W., Tschauner. O., Huang, S,. Wu, Z. Meng, Y., Bechtel. H.A., Mao, H.K. Coupled deep-mantle carbon-water cycle: Evidence from lower-mantle diamonds. *Innovation* **2**, 100117 (2021).

22. Goldschmidt, V.M. Die Gesetze der Krystallochemie. *Naturwissenschaften **21***, 477-485 (1926).

Acknowledgement: We thank N.Tomioka, an anonymous reviewer, and the editor for their helpful comments.

Funding: This work was supported by awards NSF-EAR-1838330, -EAR-1942042, EAR-1322082, the NSF Cooperative Agreement No. DMR-1644779, and the State of Florida. Use of the Advanced Photon Source and the Advanced Light Source were supported by the U. S. DOE-BES contracts DE-AC02-06CH11357 and DE-AC02-05CH11231, respectively.

Author contributions:

O.T., S.H., S.Y., M.H. participated in design, interpretation, data collection, and analysis of the reported results, and in drafting and revising the manuscript. W.L., S. G.-C., H.A.B., J.T., G.R.R. participated in data collection and revising the manuscript.

Competing interests: The authors have no competing interests.

Availability of data and materials:

Additional chemical and crystallographic information about davemaoite is provided as supplementary material. Raw data are deposited at Dryad. Crystallographic and chemical information on type davemaoite are deposited with the ICSD database. The type material is deposited with the NHMLA under accession number 74541.